HHS Public Access

Author manuscript

Biochem Biophys Res Commun. Author manuscript; available in PMC 2019 November 30.

Published in final edited form as:

Biochem Biophys Res Commun. 2018 November 30; 506(3): 463–470. doi:10.1016/j.bbrc.2018.10.073.

Stasimon/Tmem41b localizes to mitochondria-associated ER membranes and is essential for mouse embryonic development

Meaghan Van Alstyne[a,b], **Francesco Lotti**[a,b], **Andrea Dal Mas**[a,b], **Estela Area Gomez**[a,c], and **Livio Pellizzoni**[a,b,*]

[a]Center for Motor Neuron Biology and Disease, Columbia University, New York, NY, 10032, USA

[b]Department of Pathology and Cell Biology, Columbia University, New York, NY, 10032, USA

[c]Department of Neurology, Columbia University, New York, NY, 10032, USA

Abstract

Stasimon (also known as Tmem41b) is an evolutionarily conserved transmembrane protein first identified for its contribution to motor system dysfunction in animal models of the childhood neurodegenerative disease spinal muscular atrophy (SMA). Stasimon was shown to be required for normal neurotransmission in the motor circuit of *Drosophila* larvae and proper development of motor axons in zebrafish embryos as well as to suppress analogous neuronal phenotypes in SMA models of these organisms. However, the subcellular localization and molecular functions of Stasimon are poorly understood. Here, we combined immunoprecipitation with mass spectrometry to characterize the Stasimon interactome in mammalian cells, which reveals association with components of the endoplasmic reticulum (ER), mitochondria, and the COPI vesicle trafficking machinery. Expanding on the interaction results, we used subcellular fractionation studies and super-resolution microscopy to identify Stasimon as an ER-resident protein that localizes at mitochondria-associated ER membranes (MAM), functionally specialized contact sites between ER and mitochondria membranes. Lastly, through characterization of novel knockout mice, we show that Stasimon is an essential gene for mouse embryonic development. Together, these findings identify Stasimon as a novel transmembrane protein component of the MAM with an essential requirement for mammalian development.

Keywords

Stasimon (Tmem41b); spinal muscular atrophy (SMA); survival motor neuron (SMN); endoplasmic reticulum (ER); mitochondria-associated membranes (MAM); coatomer complex (COPI)

*Corresponding author: Livio Pellizzoni, Center for Motor Neuron Biology and Disease, Department of Pathology and Cell Biology, Columbia University, 630 West 168TH Street, New York, NY, 10032. Phone: +1 212-305-3046; lp2284@cumc.columbia.edu.

Conflicts of interest

The authors declare that they have no conflict of interest.

1. Introduction

Spinal muscular atrophy (SMA) is an inherited neuromuscular disorder caused by ubiquitous reduction in the levels of the survival motor neuron (SMN) protein [1]. SMN is part of a protein complex that functions in the assembly of ribonucleoproteins required for pre-mRNA splicing [1], and SMN-dependent splicing dysregulation of specific genes has been causally linked to select pathogenic events in animal models of SMA [2, 3]. The study of proximal target genes of SMN deficiency that contribute to the SMA phenotype affords unique opportunities to discover novel aspects of basic neurobiology as well as disease mechanisms.

A prominent example is *Stasimon* (also known as *Tmem41b*), a novel gene we discovered as a target of splicing dysfunction induced by SMN deficiency in both cellular and animal models of SMA [3]. Functional studies showed that Stasimon is normally required for synaptic transmission in motor circuit neurons that provide excitatory drive to motor neurons in *Drosophila* larvae as well as for motor axon outgrowth during zebrafish development [3]. Importantly, not only does its loss of function elicit neuronal phenotypes that mirror aspects of SMN deficiency *in vivo* [3,4], but Stasimon restoration corrects neurotransmission deficits in the motor circuit of *Drosophila* SMN mutants and aberrant motor neuron development in SMN-deficient zebrafish embryos [3]. These studies provided first proof-of-concept causally linking the defective splicing of a gene with important neuronal functions to specific phenotypic consequences of SMN deficiency in animal models of SMA. However, the localization and function of Stasimon as well as its requirement in the mammalian system remain poorly understood.

Stasimon is a ubiquitously expressed gene with particularly high levels in the *Drosophila* and mouse central nervous system (CNS) that encodes an evolutionarily conserved protein containing six transmembrane domains [3]. Here, we investigated the Stasimon interactome and found a network of interactions with cellular components of the endomembrane system and in particular, with the endoplasmic reticulum (ER), mitochondria, and the COPI vesicle trafficking machinery [5]. Importantly, we also found that Stasimon is an ER-resident protein that localizes at specialized sites of juxtaposition between ER and mitochondria known as mitochondrial-associated ER membranes (MAM) [6]. Lastly, analysis of novel knockout mice showed that *Stasimon* is an essential gene required for mouse embryonic development.

2. Materials and methods

2.1. DNA constructs

The open reading frames of human (NM_015012.3) and mouse (NM_153525.5) Stasimon were PCR amplified from plasmids purchased from OriGene and cloned into the BglII and HindIII sites of pEGFP-C1 (Clontech) to generate N-terminally tagged GFP fusions. The plasmid for expression of mCherry-tagged mouse Calnexin was a gift from Franck Polleux [7]. The identity of all constructs was confirmed by DNA sequencing.

2.2. Cell lines and treatments

Human HEK293 cells and mouse NIH3T3 fibroblasts were grown in DMEM with high glucose (Invitrogen) containing 10% of FBS (HyClone), 2 mM glutamine (Gibco), and 1% penicillin and streptomycin (Gibco). HEK293 and NIH3T3 cells were transfected using the CalPhos mammalian transfection kit (Clontech) and Lipofectamine 3000 (Invitrogen), respectively, and processed 72 h after transfection.

2.3. Immunoprecipitation

Protein extracts were prepared by resuspending HEK293 cells in ice-cold lysis buffer (10 mM Tris/Cl pH 7.5; 150 mM NaCl; 0.5 mM EDTA; 0.5% NP-40) supplemented with protease and phosphatase inhibitors (Roche), followed by passing through a 27-gauge syringe five times. Following centrifugation at 4°C for 15 min at 12,000 g, the protein supernatant was collected, diluted to adjust detergent concentration to binding buffer (10 mM Tris/Cl pH 7.5; 150 mM NaCl; 0.5 mM EDTA; 0.1% NP-40), and cleared through a 45 mm filter prior to addition to GFP-Trap agarose beads (Chromotek). Incubation was carried out at 4°C for 1 h, followed by five washes with 1 ml of ice-cold binding buffer. Proteins were eluted in SDS/PAGE sample buffer prior to downstream applications.

2.4. Mass spectrometry and bioinformatics

Protein identification by liquid chromatography coupled to tandem mass spectrometry (LC MS/MS) was carried out at the Proteomics Shared Resource in the Herbert Irving Comprehensive Cancer Center of Columbia University. GFP-Trap immunoprecipitates were separated on 4–12% gradient gels, followed by in-gel digestion with trypsin. The resulting peptides were processed using a Dionex Ultimate 3000 Nano liquid chromatography system, and electrosprayed into an Orbitrap Fusion Tribrid mass spectrometer equipped with an EASY-Spray source (Thermo Scientific). Tandem mass spectra were analyzed using the Proteome Discoverer 1.4 software (Thermo Finnigan) to search the human Uniprot protein database (September 2014 release). SEQUEST search results from Proteome Discoverer were further analyzed by Scaffold (Proteome Software Inc.) with protein and peptide false discovery rates set at 1% to generate the protein list and spectral counts shown in Supplementary Table 1. Gene ontology analysis was performed using DAVID version 6.7. Functional protein association networks were analyzed using STRING version 10.5.

2.5. Organelle fractionation

Purification of mitochondria, ER and MAM was performed as previously described [8,9]. HEK293 cells transfected with GFP and GFP-STAS were homogenized in isolation buffer (250 mM mannitol, 5 mM HEPES pH 7.4, and 0.5 mM EGTA). The homogenate was centrifuged for 5 min at 600 g to remove cells debris and nuclei. The supernatant was then centrifuged for 15 min at 10,500 g to yield the ER/microsomal fraction (supernatant) and the crude mitochondrial fraction (pellet). The supernatant was further centrifuged for 1 h at 100,000 g to pellet the ER/microsomal fraction. The crude mitochondrial fraction was layered on a 30% Percoll gradient, ultracentrifuged for 30 min at 95,000 g, and the upper (MAM) and lower (mitochondria free of ER) layers were collected. The upper layer fraction was then centrifuged at 100,000 g for 1 h and the resulting MAM pellet was resuspended in

isolation buffer. The lower layer fraction was diluted fivefold with isolation buffer and washed twice by centrifugation at 6,300 g for 10 min, after which pure mitochondria were resuspended in isolation buffer. All fractions were quantitated for total protein content using the Bradford system (BioRad).

2.6. Mice and genotyping

All mouse work was performed in accordance with the NIH Guidelines on the Care and Use of Animals and approved by the IACUC committee of Columbia University. Heterozygous mice harboring the gene trapped Tmem41b$^{Gt(OST208407)Lex}$ knockout allele in a 129S5/SvEvBrd × FVB/NJ background were obtained from Lexicon Pharmaceuticals and crossed with pure FVB mice for over ten generations. Genotyping was carried out with genomic DNA isolated from mouse tails or whole embryos by PCR amplification using primers across the integration site using a common forward primer (5'-ACCAAATAGACCGGTTCGTTATCC-3') and either a reverse primer (5'-AAAAGGACGCGCAACTACAACTACC-3') specific for the wild-type allele or a reverse primer located (5'-ATAAACCCTCTTGCAGTTGCATC-3') in the gene trap cassette for the knockout allele (see also Fig. 3A).

2.7. RNA and protein analysis

Total RNA was isolated from mouse embryos using TRIzol reagent (Invitrogen), followed by treatment with RNAse-free DNasel (Ambion) and reverse transcription using RevertAid RT Reverse Transcription Kit (ThermoFisher) with random hexamer and oligo dT primers. RT-qPCR analysis was performed using SYBR Green (Applied Biosystems) in technical triplicates for each biological replicate using primers specific for mouse Stasimon mRNA (forward: 5'-GAACGAAAAGCCTTGTGCAGAAGC-3'; reverse: 5'-TTCACCCTCTCTTCCTCACTAAGCTG-3') and Gapdh mRNA (forward: 5'-AATGTGTCCGTCGTGGAT CT GA-3'; reverse: 5'-GATGCCTGCTTCACCACCTTCT-3') as a normalizer.

For Western blot analysis, proteins were run on 12% polyacrylamide gels and transferred to nitrocellulose membranes for probing. Blocking was done in 5% milk in PBS/0.1% Tween. Primary and secondary antibodies were diluted in PBS/0.1% Tween. A list of the antibodies used is shown in Supplementary Table 2.

2.8. Immunofluorescence and confocal microscopy

NIH3T3 fibroblasts were fixed in 4% PFA for 15 min, then permeabilized with 0.5% Triton-X 100 in PBS for 10 min at room temperature. Samples were blocked in 3% BSA/0.05% sodium azide in PBS for 1 h, and incubated with primary antibodies in blocking buffer for 2 h. Following three 5 min washes, coverslips were incubated with secondary antibodies and DAPI diluted in blocking buffer for 1 h, washed three times, and mounted using ProLong Gold Antifade Mountant (Thermo Fisher). Cells were imaged with a Leica SP8 confocal microscope using a 63X objective. A list of the antibodies used is shown in Supplementary Table 2.

2.9. Structured illumination microscopy (SIM)

Cells plated on High-performance coverslips (Zeiss) were imaged on a Nikon Ti Eclipse inverted microscope with a SIM illuminator and iXon Ultra 897 camera (Andor) using an apo TIRF 100X oil immersion objective. Image reconstruction was performed with NIS-Elements software (Nikon). Reconstruction parameters were set as follows. Illumination modulation contrast of 2 for all channels. High-resolution noise suppression of 0.33, 0.29 and 0.10 for 561, 488 and 405 channels, respectively. Out of focus blur suppression of 0.26, 0.28 and 0.23 for 561, 488 and 405 channels, respectively.

3. Results

3.1. Analysis of the Stasimon interactome reveals association with the ER, mitochondria and the COPI complex

We sought to identify proteins associated with human STASIMON (hereafter abbreviated as STAS) by proteomic approaches. To do so, we performed anti-GFP immunoprecipitation experiments using cell extracts from HEK293 transfected with either N-terminally tagged GFP-STAS or GFP alone as well as untransfected cells as negative controls followed by SDS-PAGE and silver staining (Fig. 1A). This analysis revealed the association of several proteins with GFP-STAS but not GFP, the identity of which was then determined by LC-MS/MS. We identified 152 proteins that were found specifically in GFP-STAS immunoprecipitates but not in control immunoprecipitates with GFP alone (Supplementary Table 1). Bioinformatics analysis of the STAS interactome showed that most of the proteomics hits are part of a functional interaction network that prominently features components of ER and mitochondria (Fig. 1B). This was further confirmed by gene ontology search that revealed strong enrichment for the endomembrane system and membrane organelles such as ER and mitochondria (Fig. 1C). Additionally, all the subunits (COPA, COPB1, COPB2, COPD, COPG1, COPG2, COPE) of the COPI complex involved in vesicle coating for trafficking from Golgi to ER were among the most enriched proteins in the GFP-STAS immunoprecipitates (Fig. 1B-C). To validate the proteomics results, we performed co-immunoprecipitation experiments with GFP and GFP-STAS expressed in HEK293 cells followed by Western blot analysis and confirmed the association of STAS with select, representative components of the ER and MAM (ERLIN2), mitochondria (VDAC1) and COPI complexes (COPA and COPB1) (Fig. 1D). SMN was used as a negative control and, as expected, was not found in GFP-STAS immunoprecipitates (Fig. 1D). Collectively, these experiments indicate that STASIMON associates with ER and mitochondria proteins as well as components of the COPI vesicle trafficking machinery.

3.2. Stasimon localizes to mitochondria-associated ER membranes

To further elucidate the relationship with ER and mitochondria, we first sought to determine the subcellular localization of Stasimon using biochemical fractionation of these membrane organelles. Since antibodies that detect endogenous levels of Stasimon could not be found, we relied on the analysis of HEK293 cells transfected with GFP or GFP-STAS followed by Western blot analysis. To validate the accuracy of the fractionation procedure, we tested the distribution of known markers of subcellular compartments such as TUBULIN (cytoplasm), SDHA (mitochondria), and ERLIN2 (ER and MAM), all of which displayed their expected

distribution (Fig. 2A). Remarkably, while GFP was found only in the soluble cytoplasmic fraction, GFP-STAS was prominently associated with ER-containing fractions (Fig. 2A). Furthermore, GFP-STAS was particularly enriched in the ER fractions associated with mitochondria membranes (MAM), identified by the protein ERLIN2, but was not found in purified mitochondria (Fig. 2A). Consistent with its role in retrograde vesicle trafficking from Golgi to ER [10], the COPI complex subunit COPA was found in the cytoplasmic and ER fractions but not in the MAM.

Next, we investigated Stasimon localization in mammalian cells by immunofluorescence analysis. To do so, we transiently transfected mouse NIH3T3 fibroblasts with GFP-tagged mouse Stasimon as well as mCherry-Calnexin to label the ER, and then carried out triple-label immunostaining experiments with antibodies against GFP, mCherry and mitochondria as previously described [7]. Confocal microscopy analysis showed striking co-localization of GFP-Stas with mCherry-Calnexin but not mitochondria (Fig. 2B). To gain further insight into the localization of Stasimon with respect to ER and mitochondria, we performed super-resolution imaging by SIM microscopy followed by 3D reconstruction (Fig. 2C-D). Remarkably, these experiments revealed that GFP-Stas localizes at the contact sites between the ER and mitochondria, which is also consistent with its enrichment in biochemically purified MAM fractions.

Taken together, these experiments identify Stasimon as a novel ER-resident transmembrane protein that localizes to specific lipid-raft-rich ER domains at contact sites with outer mitochondria membranes.

3.3. Stasimon knockout causes early lethality during mouse embryonic development

To study Stasimon in mouse models, we analyzed a knockout allele that was generated by insertion of a lentiviral gene trap vector in the first intron of the *Stasimon* gene (Fig. 3A), which is expected to be a complete loss of function. Although detailed phenotypic analysis was not performed, heterozygous Stas mice harboring one copy of this allele are viable and fertile. Importantly, while heterozygous crosses yielded the expected 2 to 1 ratio of heterozygotes to wild-type mice, they failed to produce any homozygous knockout offspring (Fig. 3B), revealing an essential requirement for Stasimon during mouse embryonic development. We next sought to determine the time of embryonic lethality associated with Stasimon ablation. We performed analysis at several stages during mouse gestation and were able to identify Stasimon knockout embryos in the expected Mendelian ratio at ~E8.5, but not at later stages (Fig. 3C). Stasimon knockout in E8.5 embryos was confirmed at the molecular level by both genotyping (Fig. 3D) and mRNA analysis (Fig. 3E), which showed that knockout embryos do not express Stasimon mRNA, while heterozygotes express approximately 50% of wild-type mRNA levels (Fig. 3E). Lastly, morphological assessment of E8.5 embryos showed that Stasimon knockout embryos were developmentally arrested at around E7.5 (Fig. 3F). These studies demonstrate that *Stasimon* is an essential gene whose ablation causes embryonic lethality at the post-implantation stage of mouse development.

4. Discussion

In this study, we report three main findings that are supported by a combination of biochemistry, proteomics, high-resolution microscopy and mouse genetics data: i) the association of Stasimon with ER, mitochondria and the COPI vesicle trafficking machinery; ii) the identification of Stasimon as a novel ER-resident transmembrane protein that localizes at specialized membrane contact sites between ER and mitochondria known as MAM; and iii) the essential requirement of Stasimon for mouse embryonic development. Collectively, these findings provide new insights into Stasimon biology and highlight the importance that further studies on this protein may yield for understanding MAM function, membrane trafficking and neurodegenerative disease mechanisms.

Our investigation of the Stasimon interactome uncovered a network of associations implicating biological pathways central to the functions of ER and mitochondria, and subsequent analysis highlighted its localization to the ER. Recently, two unbiased genome-wide screens for regulators of autophagy identified Stasimon as an ER-resident protein required for autophagosome formation through undefined mechanisms [11,12]. Our independent work agrees with and significantly expands these observations, showing for the first time that Stasimon is specifically localized to the specialized MAM compartment at the interface between the ER and mitochondria membranes. While these ER-mitochondria contact sites can serve as a source of membranes during early stages of autophagosome formation [13,14] – consistent with a role for Stasimon in autophagy [11,12] – the MAM is a multifunctional site involved in several additional key cellular processes [15,16]. The close juxtaposition at the MAM facilitates cross-talk between the organelles enabling phospholipid transfer and the rapid exchange of calcium, thereby playing a critical role in the maintenance of lipid homeostasis and regulation of calcium levels which can have compounding impact on mitochondrial health and bioenergetics [17,18]. Therefore, Stasimon could have broader impact on the maintenance of MAM integrity or function and potentially play a role in additional cellular processes beyond autophagy, which are regulated by these ER-mitochondria contacts. Importantly, there has been increasing evidence for a potential role of MAM dysfunction in neurodegenerative diseases such as Alzheimer’s disease and Parkinson’s disease among others [19,20]. Evidence of autophagy and proteostasis impairment as well as mitochondrial dysfunction in SMA models has also been reported [21], but MAM dysregulation has not yet been implicated in these deficits. In light of Stasimon’s link to SMA pathology [3], the emerging role in autophagy [11,12], and the localization to the MAM we report here, characterization of Stasimon’s biology in mouse models may unravel unanticipated links with MAM-associated biological processes and with both development and disease of motor circuits.

A prominent feature of the Stasimon interactome is the multisubunit COPI complex, the association of which we further confirmed biochemically and is also consistent with results of a recent study [11]. The carboxy-terminus of Stasimon contains a dilysine motif (KXKXX), a canonical consensus sequence for COPI binding enabling retrieval of ER-resident proteins by retrograde transport [10]. In our fractionation, COPA is mostly cytoplasmic and partially overlaps with Stasimon in the ER, but not in the mitochondria-associated ER membranes. It is therefore plausible, although yet to be experimentally

validated, that the Stasimon and COPI interaction is physically and functionally distinct from those in which Stasimon engages at the MAM. Interestingly, COPI has previously been implicated in SMA pathology and COPA overexpression has been shown to correct motor axon deficits induced by SMN deficiency in zebrafish embryos [22], analogous to the requirement for Stasimon in this model system [3]. While a current model proposes that COPI role in SMA involves direct binding to SMN [22], the identification of Stasimon association with COPI provides an alternative view that may reconcile these seemingly unrelated experimental observations.

Here, we demonstrate that Stasimon is an essential gene required for mouse embryonic development as ablation induces early developmental arrest. Our findings reveal that complete loss of Stasimon is not simply lethal to all cells, but halts the progression of mouse embryogenesis during a post-implantation phase likely comprised between E7.5 and E8.5 as inferred from the aberrant morphology of E8.5 knockout embryos. Although embryonic lethality is consistent with its ubiquitous expression, Stasimon's high levels of expression in the CNS also suggest a key role in neurons, consistent with its requirement for motor circuit function [3]. Unfortunately, the early embryonic lethality associated with constitutive Stasimon knockout precludes direct evaluation of its requirement for development and function of the mouse motor system, and calls for the development of conditional knockout mice.

In the future, the study of the spatial and temporal requirement for Stasimon *in vivo*, combined with further molecular characterization of its functions is likely to yield new fundamental insights into the biology of ER-mitochondria contacts, autophagy and membrane trafficking in mammalian neurons as well as mechanisms of neurodegenerative disease.

Supplementary Material

Refer to Web version on PubMed Central for supplementary material.

Acknowledgements

We are grateful to Lexicon Pharmaceuticals and the SMA Foundation for providing mice with the targeted Stasimon allele. We thank Catarina Quinzii, Franck Polleux and George Mentis for sharing reagents and helpful comments. This work was supported by the SMA Foundation and the National Institutes of Health [R21NS077038 and R01NS102451].

References

[1]. Tisdale S, Pellizzoni L, Disease Mechanisms and Therapeutic Approaches in Spinal Muscular Atrophy, J. Neurosci 35 (2015) 8691–8700. [PubMed: 26063904]

[2]. Van Alstyne M, Simon CM, Sardi SP, Shihabuddin LS, Mentis GZ, Pellizzoni L, Dysregulation of Mdm2 and Mdm4 alternative splicing underlies motor neuron death in spinal muscular atrophy, Genes Dev. 32 (2018) 1045–1059. [PubMed: 30012555]

[3]. Lotti F, Imlach WL, Saieva L, Beck ES, Hao LT, Li DK, Jiao W, Mentis GZ, Beattie CE, McCabe BD, Pellizzoni L, An SMN-dependent U12 splicing event essential for motor circuit function, Cell 151 (2012) 440–454. [PubMed: 23063131]

[4]. Imlach WL, Beck ES, Choi BJ, Lotti F, Pellizzoni L, McCabe BD, SMN is required for sensory-motor circuit function in Drosophila, Cell 151 (2012) 427–439. [PubMed: 23063130]

[5]. Beck R, Rawet M, Ravet M, Wieland FT, Cassel D, The COPI system: molecular mechanisms and function, FEBS Lett. 583 (2009) 2701–2709. [PubMed: 19631211]

[6]. Herrera-Cruz MS, Simmen T, Over Six Decades of Discovery and Characterization of the Architecture at Mitochondria-Associated Membranes (MAMs), Adv. Exp. Med. Biol 997 (2017) 13–31. [PubMed: 28815519]

[7]. Hirabayashi Y, Kwon S-K, Paek H, Pernice WM, Paul MA, Lee J, Erfani P, Raczkowski A, Petrey DS, Pon LA, Polleux F, ER-mitochondria tethering by PDZD8 regulates Ca2+ dynamics in mammalian neurons, Science 358 (2017) 623–630. [PubMed: 29097544]

[8]. Wieckowski MR, Giorgi C, Lebiedzinska M, Duszynski J, Pinton P, Isolation of mitochondria-associated membranes and mitochondria from animal tissues and cells, Nat. Protoc 4 (2009) 1582–1590. [PubMed: 19816421]

[9]. Area-Gomez E, Assessing the Function of Mitochondria-Associated ER Membranes, Methods Enzymol. (2014) 181–197.

[10]. Brandizzi F, Barlowe C, Organization of the ER-Golgi interface for membrane traffic control, Nat. Rev. Mol. Cell Biol 14 (2013) 382–392. [PubMed: 23698585]

[11]. Moretti F, Bergman P, Dodgson S, Marcellin D, Claerr I, Goodwin JM, DeJesus R, Kang Z, Antczak C, Begue D, Bonenfant D, Graff A, Genoud C, Reece-Hoyes JS, Russ C, Yang Z, Hoffman GR, Mueller M, Murphy LO, Xavier RJ, Nyfeler B, TMEM41B is a novel regulator of autophagy and lipid mobilization, EMBO Rep. 19 (2018) e45889. [PubMed: 30126924]

[12]. Morita K, Hama Y, Izume T, Tamura N, Ueno T, Yamashita Y, Sakamaki Y, Mimura K, Morishita H, Shihoya W, Nureki O, Mano H, Mizushima N, Genome-wide CRISPR screen identifies *TMEM41B* as a gene required for autophagosome formation, J. Cell Biol (2018) jcb.201804132.

[13]. Hailey DW, Rambold AS, Satpute-Krishnan P, Mitra K, Sougrat R, Kim PK, Lippincott-Schwartz J, Mitochondria Supply Membranes for Autophagosome Biogenesis during Starvation, Cell 141 (2010) 656–667. [PubMed: 20478256]

[14]. Hamasaki M, Furuta N, Matsuda A, Nezu A, Yamamoto A, Fujita N, Oomori H, Noda T, Haraguchi T, Hiraoka Y, Amano A, Yoshimori T, Autophagosomes form at ER-mitochondria contact sites, Nature 495 (2013) 389–393. [PubMed: 23455425]

[15]. Marchi S, Patergnani S, Pinton P, The endoplasmic reticulum-mitochondria connection: one touch, multiple functions, Biochim. Biophys. Acta 1837 (2014) 461–469. [PubMed: 24211533]

[16]. Wu H, Carvalho P, Voeltz GK, Here, there, and everywhere: The importance of ER membrane contact sites, Science. 361 (2018) eaan5835.

[17]. Raturi A, Simmen T, Where the endoplasmic reticulum and the mitochondrion tie the knot: The mitochondria-associated membrane (MAM), Biochim. Biophys. Acta - Mol. Cell Res 1833 (2013) 213–224.

[18]. van Vliet AR, Verfaillie T, Agostinis P, New functions of mitochondria associated membranes in cellular signaling, Biochim. Biophys. Acta - Mol. Cell Res 1843 (2014) 2253–2262.

[19]. Area-Gomez E, Schon EA, On the Pathogenesis of Alzheimer's Disease: The MAM Hypothesis, FASEB J. 31 (2017) 864–867. [PubMed: 28246299]

[20]. Paillusson S, Stoica R, Gomez-Suaga P, Lau DHW, Mueller S, Miller T, Miller CCJ, There's Something Wrong with my MAM; the ER-Mitochondria Axis and Neurodegenerative Diseases, Trends Neurosci. 39 (2016) 146–157. [PubMed: 26899735]

[21]. Chaytow H, Huang Y-T, Gillingwater TH, Faller KME, The role of survival motor neuron protein (SMN) in protein homeostasis, Cell. Mol. Life Sci 75 (2018) 3877–3894.

[22]. Li H, Custer SK, Gilson T, Hao LT, Beattie CE, Androphy EJ, α-COP binding to the survival motor neuron protein SMN is required for neuronal process outgrowth, Hum. Mol. Genet 24 (2015) 7295–7307. [PubMed: 26464491]

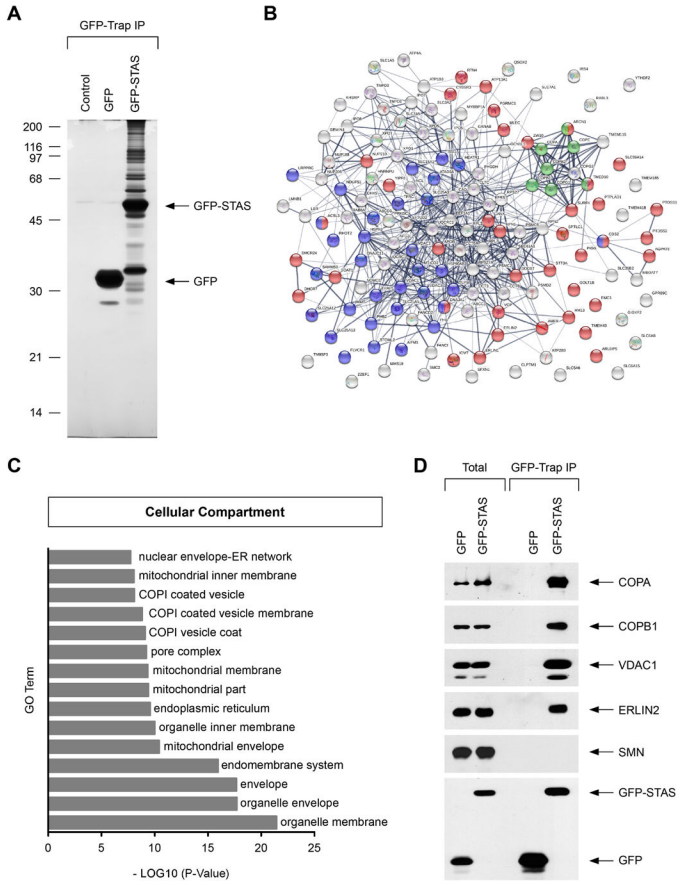

Fig. 1.

Characterization of the Stasimon interactome. (A) Silver staining of GFP-Trap immunoprecipitates from HEK293 cells either untransfected (Control) or transfected with GFP and GFP-STAS. 10% of the material used for mass spectrometry is shown. (B) Functional protein association network of specific proteins identified in GFP-STAS immunoprecipitates using STRING. Protein components of mitochondria (blue), ER (red) and COPI complex (green) are color-coded. The protein names are visible after zoom-in. (C) Gene ontology analysis of the most enriched cellular compartments associated with the specific proteins identified in GFP-STAS immunoprecipitates using DAVID. (D) Western blot analysis of GFP-Trap immunoprecipitates from HEK293 cells expressing GFP or GFP-STAS. Total represents 5% of the protein input.

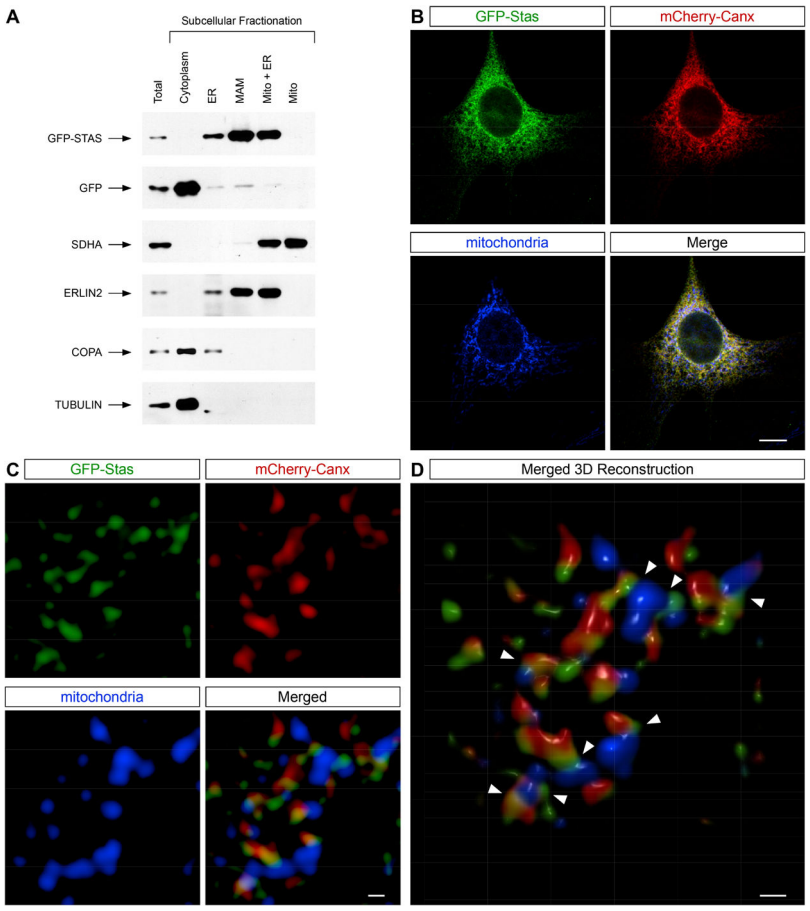

Fig. 2.

Stasimon is an ER-resident protein that localizes to the MAM. (A) Western blot analysis of the subcellular localization of GFP and GFP-STAS following biochemical fractionation of transiently transfected HEK293 cells. Equal amounts (20μg) of proteins for each fraction were analyzed. (B) Confocal imaging of NIH3T3 cells co-transfected with GFP-Stas and mCherry-Canx and immunostained with antibodies for dsRed, GFP and a cocktail of mitochondrial oxidative phosphorylation proteins (mitochondria). Scale bar, 10μm. (C) Super-resolution 3D SIM microscopy of NIH3T3 cells immunolabeled as in (B). A single plane image of all three channels and a merged image are shown. Scale bar, 0,2μm. (D) 3D reconstruction of SIM microscopy images from (C). Arrowheads indicate GFP-Stas localization at ER-mitochondria contacts. Scale bar, 0,2μm.

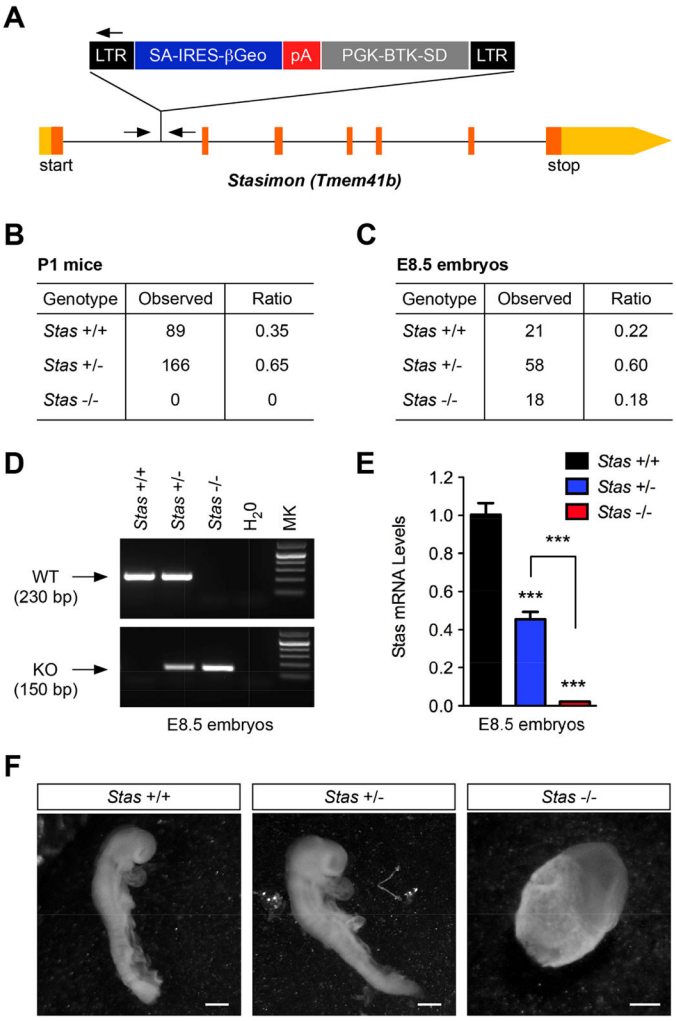

Genotype	Observed	Ratio
Stas +/+	89	0.35
Stas +/-	166	0.65
Stas -/-	0	0

Genotype	Observed	Ratio
Stas +/+	21	0.22
Stas +/-	58	0.60
Stas -/-	18	0.18

Fig. 3.

Stasimon is essential for mouse embryonic development. (A) Schematic of the Tmem41b$^{Gt(OST208407)Lex}$ knockout allele of the *Stasimon* gene. The location of genotyping primers across the insertion site in intron 1 and on the gene-trap vector are shown. (B) Ratio and number of mice with the indicated genotypes observed at postnatal day 1 (P1) from crosses of Stasimon heterozygous mice. (C) Ratio and number of E8.5 embryos with the indicated genotypes from crosses of *Stasimon* heterozygous mice. (D) Genomic PCR of wild-type (WT) and knockout (KO) alleles from E8.5 embryos of the indicated genotypes. (E) RT-qPCR of Stasimon mRNA levels normalized to Gapdh mRNA expression in E8.5 embryos of the indicated genotypes. Data represent mean and SEM (n=3). Statistics were performed with oneway ANOVA with Tukey's *post hoc* test (*** $P < 0.001$). (F) Images of E8.5 embryos of the indicated genotypes. Scale bars, 50μm.